Supporting Information

Supramolecular oligourethane gel as a highly selective fluorescent "on-off-on" sensor for ions

Yulin Feng,[‡,a] Nan Jiang,[‡,a] Dongxia Zhu,*[,a] Zhongmin Su*[,a] and Martin R. Bryce*[,b]

[a] Key Laboratory of Nanobiosensing and Nanobioanalysis at Universities of Jilin Province,

Department of Chemistry, Northeast Normal University, 5268 Renmin Street, Changchun,

Jilin Province 130024, P. R. China

[b] Department of Chemistry, Durham University, Durham, DH1 3LE, UK

E-mail: m.r.bryce@durham.ac.uk

Table of Contents:

1. Experimental details

2. Structural characterization of OU

3. Photophysical properties of OU

1. Experimental details

General:

Materials obtained from commercial suppliers were used without further purification unless otherwise stated. All glassware, syringes, magnetic stirring bars, and needles were thoroughly dried in a convection oven. ^1H NMR spectra were recorded at 25 ℃ on a Varian 500 MHz spectrometer and were referenced internally to the residual proton resonance in DMSO-d_6 (δ 2.5 ppm). The molecular weight of the polymer was calculated from its ^1H NMR spectrum.[S1] The emission spectra were recorded using a F-7000 FL spectrophotometer. The infrared spectral data of the oligourethane were recorded using a Nicolet 6700-FTIR spectrometer. UV-vis absorption spectra were obtained by a Shimadzu UV-3100 spectrophotometer. X-ray diffraction (XRD) patterns of the samples were obtained with a Rigaku Dmax 2000. The scanning electron microscopy (SEM) images were obtained using a HITACHI SU8010.

Cation and anion sensing studies:

Stock solutions of various ions, including Na^+, Ca^{2+}, Co^{2+}, Cu^{2+}, Mn^{2+}, Ni^{2+}, Cr^{3+}, La^{3+}, Fe^{3+}, Sr^{2+}, Ce^{3+}, Ag^+, Al^{3+}, Mg^{2+}, Cd^{2+}, Pb^{2+}, Fe^{2+}, HSO_4^-, ClO_4^-, I^-, CN^-, PF_6^-, F^-, Cl^-, Br^-, NO_3^-, AcO^- (using nitrate salts as the cation sources and tetrabutylammonium salts as the anion sources) were prepared in water at concentrations of 0.2 M, respectively. The cations sensing measurements of **OUG** (10%) were carried out by sequentially adding a different cationic solution to immerse gels in a ceramic colorimetric dish. The fluorescence spectra of the resultant metallogels were then recorded at room temperature. The fluorescence measurements of **OUFeG** were carried out by sequentially adding a different anionic solution. The measuring procedures for **OUFeG** were the same as for **OUG**.

Method for detection limit calculation:

The limit of detection (LOD) was calculated using the equation $3\delta/S$, where δ is the standard deviation (SD) for **OUG** intensity in the absence of Fe^{3+} on the **OUFeG** intensity in the absence of anions. S denotes the slope of the curve.

Urea Addition Experiment:

A gel (10 wt %) in DMF was prepared and then urea (10 equiv.) was added to the gel vial and then the vial was heated to obtain a clear solution and then cooled to room temperature. No gel was formed after urea addition.

Calculation method of absorbing rate:

The absorbing rate was calculated by the following equation:

Absorbing rate % = (1 - c/c_0) $\times$ 100%

where c_0 is the initial metal ion concentration in the absence of the **OUG**, c is the metal ion concentration after the treatment of the corresponding analyte.

Synthesis of OU:

OU was synthesized by condensation polymerization between hexamethylene diisocyante (A) and 4,4'-dihydroxybenzophenone (B) in the presence of polyethylene glycol monomethyl ether (PEG-200) (C) as the end-capper and 1,4-diazabicyclo[2.2.2]octane (DABCO) as the catalyst (Scheme S1). To make sure that the oligourethane chains were capped both ends by PEG, specific amounts were used of the two monomers and the end-capper satisfying the equation: $2N_A = 2N_B + N_C$, where N is the mole fraction of each component.
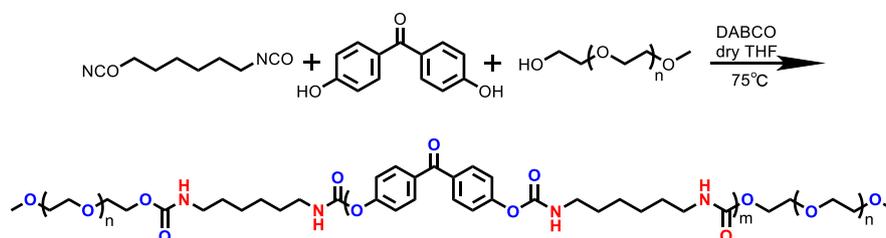
Scheme S1 Synthesis of **OU**.

A mixture of 4,4'-dihydroxybenzophenone (2.62 mmol), DABCO (0.107 mmol) and anhydrous THF (8 mL) were added to a dried two-neck round-bottom flask. When they had almost dissolved into a transparent solution, PEG-200 (1.98 mmol) and hexamethylene

diisocyanate (3.61 mmol) were added to the mixed system in turn. The solution was heated at 75 °C for 8 h under nitrogen atmosphere until the clear solution became viscous, indicating polymerization had occurred. After cooling to room temperature, the crude product was washed with ethyl alcohol to give a white solid. This product was dried under vacuum for 24 h to obtain the resulting OU. Yield: 68%. ^{1}H NMR (500 MHz, DMSO-d_6, δ [ppm]): 7.2/7.9 (s, 2H, -NH), 7.6-7.8 (broad, 4H), 7.23-7.34 (broad, 3H), 6.85-6.93 (broad, 1H)，4.04 (s, 4H)，3.40-3.61 (broad, PEG protons), 3.33 (s, 6H, PEG terminal -OCH$_3$ protons), 2.91-3.14 (broad, 4H), 0.7-1.6 (broad, 8H). FTIR: 3323 cm^{-1} (N-H), 2936 and 2860 cm^{-1} (-CH$_2$ -asymmetric and symmetric stretch), 1706 cm^{-1} (C=O), 1163 cm^{-1} (C-O-C stretch PEG).

It is known that the number-average molecular weight (M_n) of end-functional polymers/oligomers can be obtained accurately using ^{1}H NMR spectroscopy for end-group analysis.[S2] OU was characterized by ^{1}H NMR spectra, in which all peaks could be assigned unambiguously (see above description). By comparing the integration of the peak for H$_e$ (terminal groups -CH$_3$ protons) and H$_c$ (repeating unit CH$_2$ protons), the degree of polymerization (DP) was found to be 3.6; and M_n was found to be 1814 g mol^{-1} according to the following equation:

$$\overline{M}_n = M\,\overline{DP} + 2M_{EG}$$

where M and M_{EG} are the molecular weights of the repeat unit and end-group, respectively.

Table S1: Gelation Properties of **OUG** in Various Solvents.

Entry	Solvent	State[a]	CGC[b] (%)	T_{gel}[c]
1	Water	P	\	\
2	Acetone	P	\	\
3	Methanol	P	\	\
4	Ethanol	P	\	\
5	Isopropanol	P	\	\

6	Acetonitrile	P	\	\
7	THF	P	\	\
8	DMF	G	4	85-87
9	N-propanol	P	\	\
10	CCl_4	P	\	\
11	N-hexane	P	\	\
12	Diethyl ether	P	\	\
13	CH_2Cl_2	P	\	\
14	$CHCl_3$	P	\	\
15	CH_2ClCH_2Cl	P	\	\
16	Petroleum Ether	P	\	\
17	Ethyl acetate	P	\	\
18	DMSO	G	4.5	60-62
19	N-butyl Alcohol	P	\	\
20	Methylbenzene	P	\	\
21	Hexamethylene	P	\	\

[a] G, P and S denote gelation, precipitation and solution, respectively;

[b] The critical gelation concentration (wt %, 10 mg/mL = 1.0 %);

[c] The gelation temperature (°C).
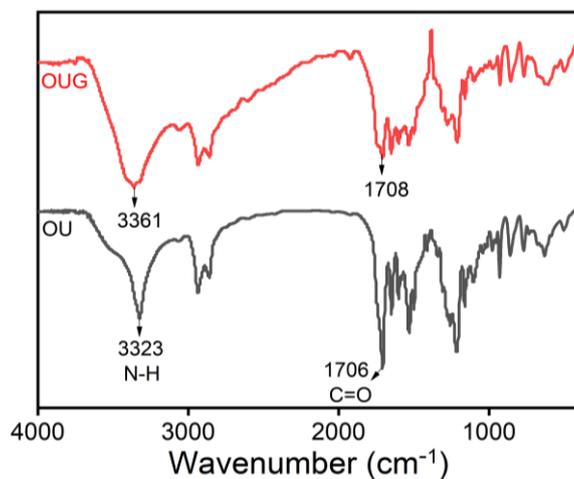
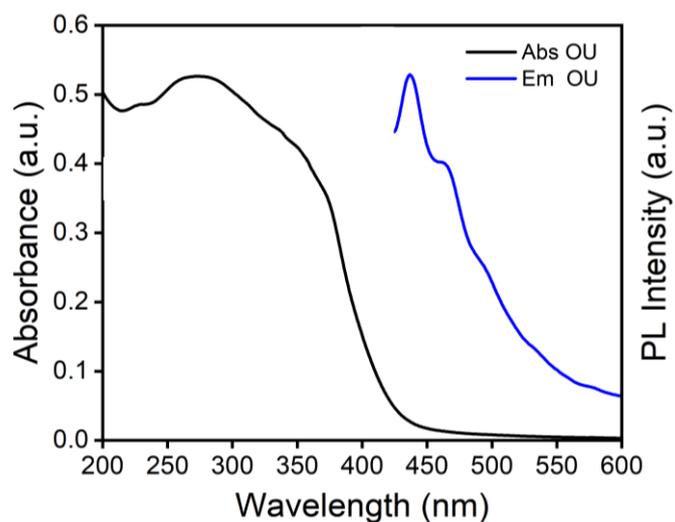**Fig. S1** FTIR spectra of OU and **OUG**.

Fig. S2 Absorption and emission spectra of OU in the solid state at room temperature.
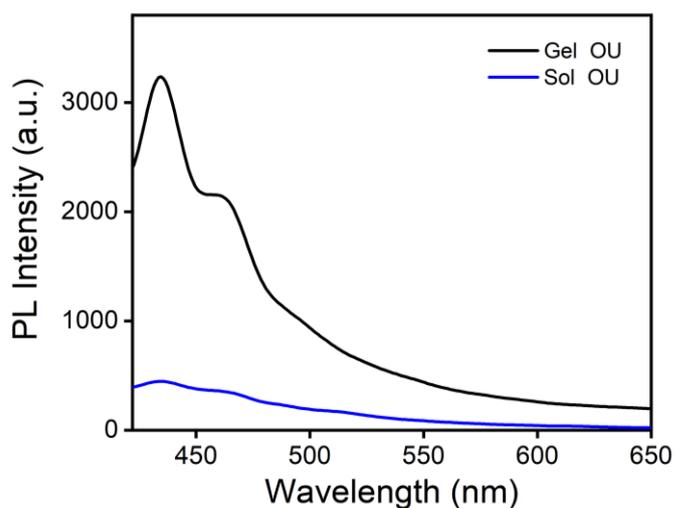

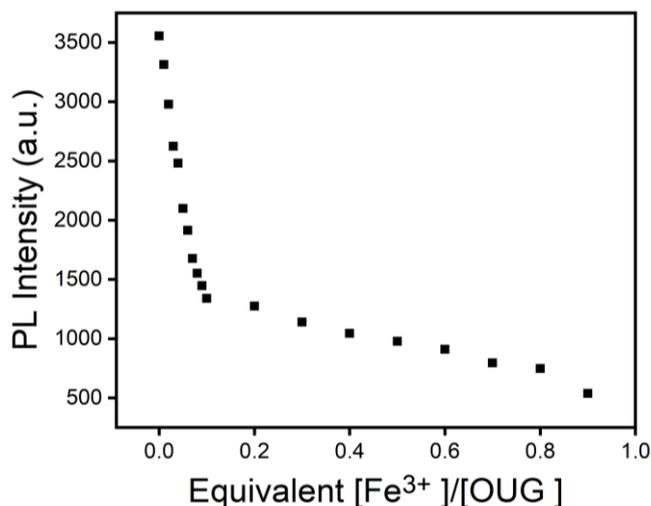**Fig. S3** PL spectra of OU in gel and sol states.

Fig. S4 A plot of emission at 384 nm versus number of equivalents of Fe^{3+}.

The result of the analysis is as follows:

Linear Equation: Y = -27282.37X + 3807.94

$R^2 = 0.9922$

$S = 2.7282 \times 10^{10}$

$$\delta = \sqrt{\frac{\sum_{i=1}^{N}(F_i - \overline{F})}{N-1}} = 53.56$$

(N = 20)   K = 3

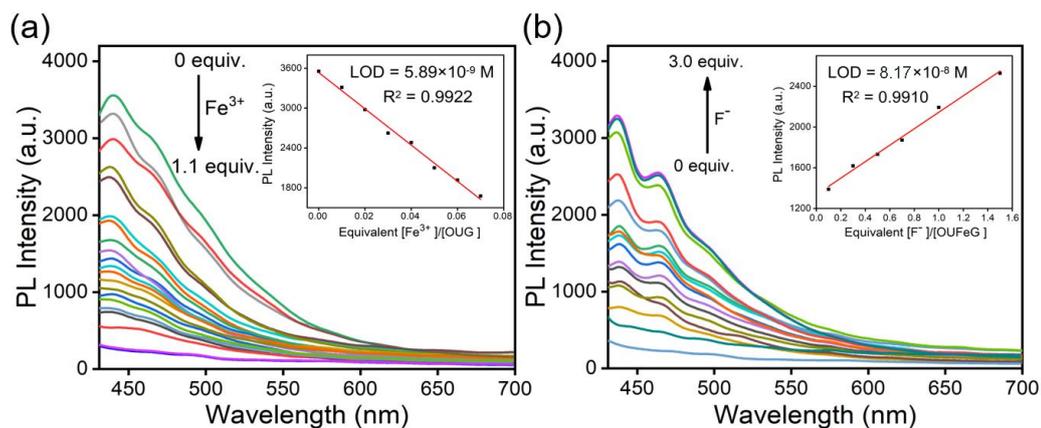$LOD = K \times \delta/S = 5.89 \times 10^{-9}$ M

Fig. S5 (a) Fluorescence spectra of **OUG** with increasing amounts of Fe^{3+}. (b) Fluorescence spectra of **OUFeG** with increasing concentrations of F^- (λ_{ex} = 384 nm). Insert: The corresponding linear graph.

Table S2 Comparison of the Analytical Performance of the Fluorescence Sensing Systems for ions.

ions	Refs	Fluorescent materials	LOD
Fe^{3+}	S3	Carbon Nanodots	4×10^{-8} M
	S4	MIL-53 (Al)	9×10^{-7} M
	S5	Nap-Glc	4.27×10^{-8} M
	S6	Furfuran-based Rhodamine B Fluorescent Chemosensor	2.5×10^{-8} M
	S7	Ultrabright N/P Codoped Carbon Dots	3.3×10^{-7} M
	S8	Rhodamine B Derivative-functionalized Graphene Quantum Dots	2×10^{-8} M
	S9	Eu(III)-functionalized MIL-124	2.8×10^{-7} M
	This work	**Oligourethane Gel (OUG)**	**5.89×10^{-9} M**
F^-	S10	Luminescent Iridium(III) Chemosensor	7.2×10^{-7} M
	S11	Reactive Fluorogenic Probes	1.14×10^{-6} M
	S12	2-(hydroxy)-naphthyl Imino Functionalized Pillar[5]arene	1.34×10^{-7} M
	S13	Coumarin-based Colorimetric and Fluorescent Chemosensor	9.2×10^{-6} M
	S14	Boron-dipyrromethene Chemosensor	9.3×10^{-8} M
	This work	**Oligourethane Gel (OUG)**	**8.17×10^{-8} M**
HSO_4^-	S15	Coumarin-based Fluorescent Sensor	3.75×10^{-6} M
	S16	Styrylindolium Dyes	1.0×10^{-6} M
	S17	Schiff Base	2.4×10^{-7} M

	S18	BODIPY-derived Multi-channel Polymeric Chemosensor	1.12×10^{-6} M
	S19	Benzothiazole Based Schiff-base-A	3.2×10^{-8} M
	This work	**Oligourethane Gel (OUG)**	**1.16×10^{-8} M**

Table S3 The AAS data of gel **OUG** with Fe^{3+}.

Ion	Initial concentration (M)	Residual concentration (M)	Absorbing rate %
Fe^{3+}	1.0×10^{-5}	2.5×10^{-7}	97.5
Fe^{3+}	1.0×10^{-4}	1.05×10^{-5}	89.5
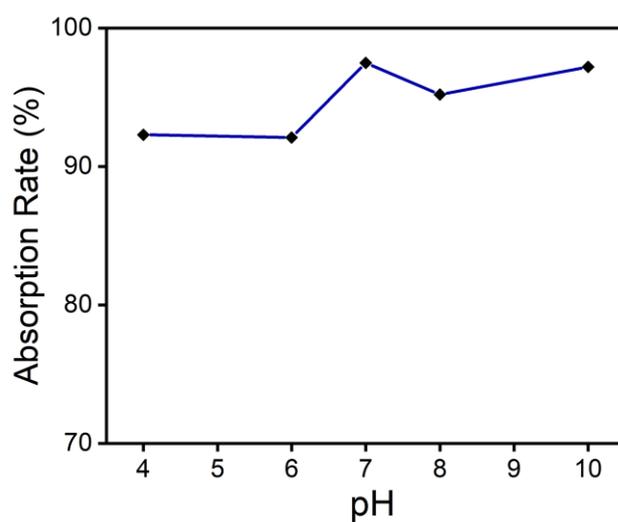
Fig. S6 The absorption rates of **OUG** toward Fe^{3+} (1×10^{-5} mol L^{-1} in 10 mL water) at different pH.
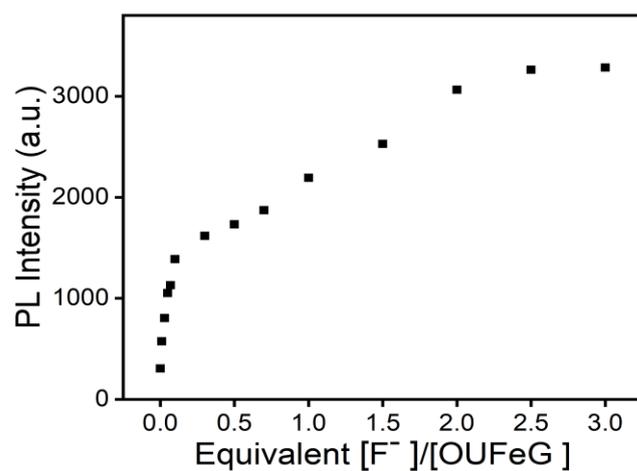
Fig. S7 A plot of emission at 384 nm versus number of equivalents of F⁻.

The result of the analysis as follows:

Linear Equation: Y = 808.49X + 1336.53

$R^2 = 0.9910$

$S = 8.0849 \times 10^8$

$$\delta = \sqrt{\frac{\sum\limits_{i=1}^{N}(F_i - \overline{F})}{N-1}} = 22$$
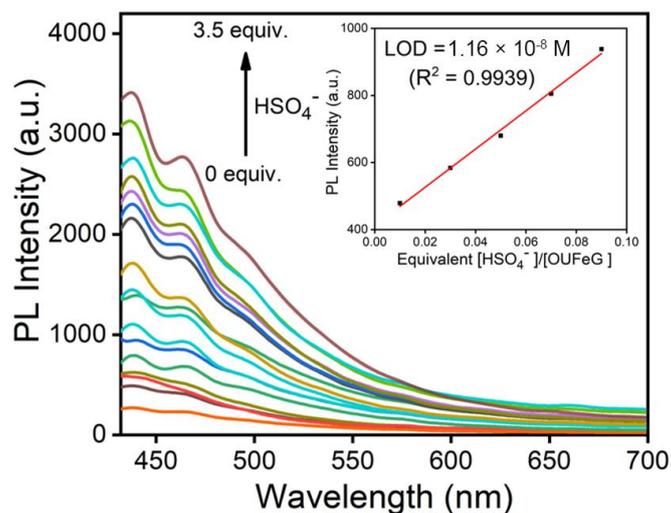
(N = 20)   K = 3

LOD = K × δ/S = 8.17×10^{-8} M

Fig. S8 Fluorescence spectra of **OUG** with increasing concentrations of HSO_4^- (λ_{ex} = 384nm). Insert: The corresponding linear graph.
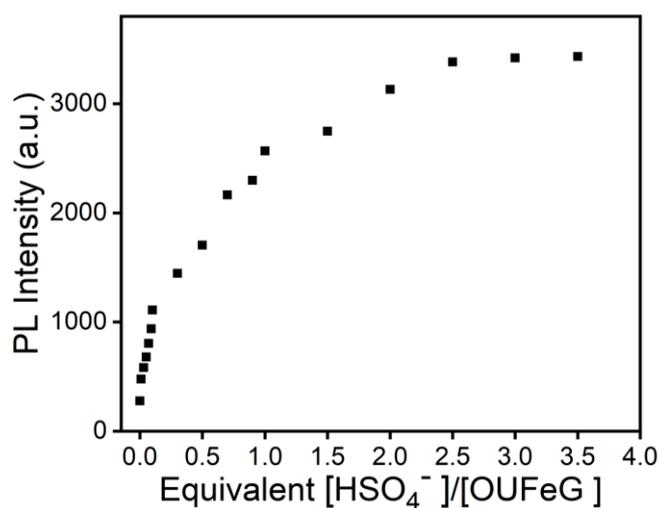

Fig. S9 A plot of emission at 384 nm versus number of equivalents of HSO_4^-.

Linear Equation: Y = 5695X + 412.45

R^2 = 0.9939

S = 5.695×10^9

$$\delta = \sqrt{\frac{\sum_{i=1}^{N}(F_i - \overline{F})}{N-1}} = 22$$

(N = 20)   K = 3

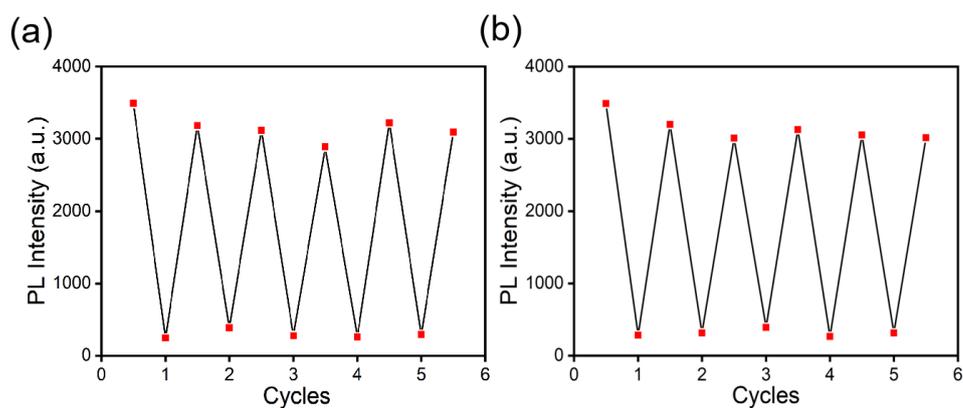LOD = K $\times$ δ/S = 1.16×10^{-8} M

Fig. S10 Fluorescent "on-off-on" cycles of **OUG**, controlled by the alternating addition of (a) Fe^{3+} and F^-, (b) Fe^{3+} and HSO_4^- (λ_{ex} = 384 nm).
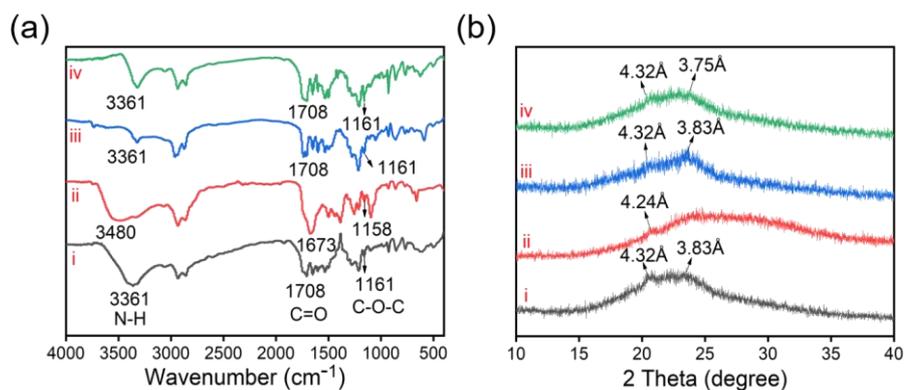

Fig. S11 (a) FTIR spectra of of (i) **OUG** (ii) **OUFeG** (iii) **OUFeG** + HSO_4^- and (iv) **OUFeG** + F^-, (b) powder XRD patterns of (i) **OUG** (ii) **OUFeG** (iii) **OUFeG** + HSO_4^- and (iv) **OUFeG** + F^-.

References

S1   N. Jiang, G. Li, W. Che, D. Zhu, Z. Su and M. R. Bryce, *J. Mater. Chem. C*, 2018, **6**, 11287-11291.

S2   M. J. Robb, D. Montarnal, N. D. Eisenmenger, S.-Y. Ku, M. L. Chabinyc, and C. J. Hawker, *Macromolecules*, 2013, **46**, 6431−6438.

S3   P. Miao, Y. Tang, K. Han and B. Wang, *J. Mater. Chem. A*, 2015, **3**, 15068-15073.

S4   C.-X. Yang, H.-B. Ren and X.-P. Yan, *Anal. Chem.*, 2013, **85**, 7441-7446.

S5   F. Liu, P. Tang, R. Ding, L. Liao, L. Wang, M. Wang and J. Wang, *Dalton Trans.*, 2017, **46**, 7515-7522.

S6   T. Zhou, X. Chen, Q. Hua, W. Lei, Q. Hao, B. Zhou, C. Su, and X. Bao, *Sens. Actuators, B*, 2017, **253**, 292-301.

S7   J. Shangguan, J. Huang, D. He, X. He, K. Wang, R. Ye, X. Yang, T. Qing, and J. Tang, *Anal. Chem.*, 2017, **89**, 7477-7484.

S8   R. Guo, S. Zhou, Y. Li, X. Li, L. Fan, and N. H. Voelcker, *ACS Appl. Mater. Interfaces*, 2015, **7**, 23958-23966.

S9   X.-Y. Xu and B. Yan, *ACS Appl. Mater. Interfaces*, 2015, **7**, 721-729.

S10   J.-B. Liu, W. Wang, G. Li, R.-X. Wang, C.-H. Leung, and D.-L. Ma, *ACS Omega*, 2017, **2**, 9150-9155.

S11   J. Hu, T. Liu, H.-W. Gao, S. Lu, K. Uvdal, and Z. Hu, *Sens. Actuators, B*, 2018, **269**, 368-376.

S12   W. Zhu, H. Fang, J.-X. He, W.-H. Jia, H. Yao, T.-B. Wei, Q. Lin and Y.-M. Zhang, *New J. Chem.*, 2018, **42**, 11548-11554.

S13   S. Biswas, M. Gangopadhyay, S. Barman, J. Sarkar, and N. P. Singh, *Sens. Actuators, B*, 2016, **222**, 823-828.

S14   S. Madhu and M. Ravikanth, *Inorg. Chem.*, 2014, **53**, 1646-1653.

S15   H. J. Kim, S. Bhuniya, R. K. Mahajan, R. Puri, H. Liu, K. C. Ko, J. Y. Lee and J. S. Kim, *Chem. Commun.*, **2009**, 7128-7130.

S16   J. Chang, Y. Lu, S. He, C. Liu, L. Zhao and X. Zeng, *Chem. Commun.*, 2013, **49**, 6259-6261.

S17   C.-Y. Lin, K.-F. Huang, and Y.-P. Yen, *Spectrochim. Acta, Part A*, 2013, **115**, 552-558.

S18   U. Haldar and H.-i Lee, *Polym. Chem.*, 2018, **9**, 4882-4890.

S19   I. Kaur, A. Khajuria, P. Ohri, P. Kaur, and K. Singh, *Sens. Actuators, B*, 2018, **268**, 29-38.